INFLUENCE OF RANDOM LOCAL LOAD SHARING ON TENSILE BEHAVIOR OF MULTIFILAMENT TOWS AND CERAMIC MATRIX COMPOSITE FAILURE

V. Calard and J. Lamon

Laboratoire des Composites Thermostructuraux
UMR 5801 (CNRS-SNECMA-CEA-University of Bordeaux 1)
3 Allée de la Boétie
33600 Pessac, France
lamon@lcts.u-bordeaux.fr

ABSTRACT

The paper compares experimental data and theory on the tensile behavior and strength of multifilament tows. Tow tensile behavior was predicted from single fiber properties using classical bundle theory. Then the contribution of random local load sharing was modelled. This analysis was applied to SiC multifilament tows (Nicalon and Hi-Nicalon, Nippon Carbon Co., Japan).

1. INTRODUCTION

Fibre strength is a factor of primary importance in ceramic matrix composite strength, since fibres are expected to increase the resistance to failure. Furthermore, multifilament tows appear to be fundamental entities in textile composites, that dictate ultimate failure [1]. Data on the resistance of single filaments and multifilament tows are required for prediction of ultimate failure of composites.

Multifilament tows exhibit a non-linear tensile behavior as a result of individual fiber breaks that don't cause tow failure: this behavior is essentially elastic damageable even in the presence of brittle filaments. The tensile behavior of tows containing parallel and non contacting fibers has been modelled by several authors [2-5] on the basis of equal load sharing (ELS) concept: when a fiber breaks, the load is shared by the surviving fibers.

Local load sharing (LLS) is essentially observed in those fiber reinforced composites for which the matrix is able to transfer loads, and contributes to local stress concentrations around the broken fibers (polymer matrix composites). Imperfect or random local load sharing (RLLS) [6] may be expected within tows during individual fiber breaks, as a result of local fiber frictions [7] or dynamic effects associated to propagation of strain waves, and also in ceramic matrix composites after saturation of matrix cracking. RLLS involves less fibers than LLS does since fiber stress redistribution depends on the degree of interaction of the breaking fiber with its neighbours.

The present paper examines the experimental tensile behavior of multifilament tows with respect to theory. A certain emphasis is placed on the influence of random local load sharing (RLLS) on the ultimate failure of tows.

2. MODELS, SIMULATIONS AND EXPERIMENTAL PROCEDURES

2.1- Classical bundle theory

The bundle models are based upon the following hypotheses [2, 3] : the bundle contains N_t identical and parallel fibers (Radius R_f, length l), and the statistical distribution of fiber strengths is described by the Weibull model :

$$P(\sigma) = 1 - \exp[-\frac{V}{V_o}(\frac{\sigma}{\sigma_o})^m] \qquad (1)$$

Where V is the volume subject to a uniform stress, V_o is the reference volume ($V_o = 1$ m^3), m and σ_o are fibers statistical parameters.
When a fiber fails during a tensile test, equal load sharing is assumed. This means that the load is carried equally by all the surviving fibers.
Under strain-controlled conditions, there is no overloading of surviving fibers when a fiber fails. Failure is a stable phenomenon. Tow tensile behavior is decribed by the following equation :

$$F(\varepsilon) = N_t S_f E\varepsilon \exp[-\frac{V}{V_o}(\frac{E\varepsilon}{\sigma_o})^m] \qquad (2)$$

where S_f is the fiber cross sectional area ($S_f = \pi R_f^2$). E is fiber Young's modulus and ε is the applied strain.
The maximum force is given by the following equation, under load – and strain-controlled conditions [6] :

$$F_{max} = N_t (1 - \alpha(\sigma_{max})) S_f \sigma_{max} \qquad (3)$$

where $\alpha(\sigma_{max})$ is the critical number of fibers broken individually and σ_{max} is the stress at maximum force. The corresponding coefficient of variation is [6] :

$$C_v(F_{max}) = \frac{S(F_{max})}{E(F_{max})} = \sqrt{\frac{\alpha(\sigma_{max})}{N_t(1-\alpha(\sigma_{max}))}} \qquad (4)$$

where E ( ) is the expectation and S^2 ( ) is the variance. Note that $C_v(F_{max})$ is small when N_t is large. Therefore, the maximum forces F_{max} should not exhibit a significant scatter.

2.2- Numerical simulation of tow tensile behavior

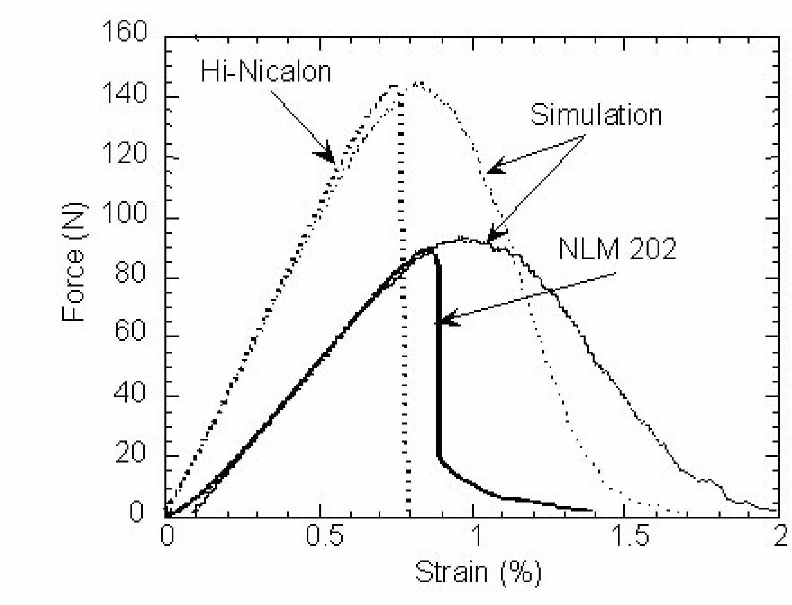

Figure 1 : Typical force-strain behavior obtained under strain-controlled conditions for NLM 202 and Hi-Nicalon tows and curves predicted assuming ELS [6].

Each fiber within a tow was assigned a strength that was derived from a random number x using equation (5) :

$$x_i = P(\sigma_i) \tag{5}$$

where x_i is a number generated randomly and associated to fiber i ($0 < x_i < 1$). σ_i is the strength of fiber i. P( ) is the failure probability of a single fiber given by equation (1). Failure of a fiber occurs when $\sigma_i \leq \sigma$, where σ is the stress operating on the fibers.
Under load-controlled loading conditions, when a fiber breaks, the load that it was carrying is shared by surviving fibers. The resulting new stress-state is compared to fiber strengths to identify whether other fibres can fail. The applied force is increased only when further fiber failures cannot occur under the current conditions.
Under strain-controlled conditions, there is no overloading of the surviving fibers when a fiber breaks.
In equal load sharing conditions, the load is carried equally by the surviving fibers. Forces and deformations are related by the following equation :

$$\varepsilon = \frac{F}{E(N_t - N)S_f} \tag{6}$$

2.3- Modelling of random local load sharing
Local load sharing in composites with a compliant matrix has been studied in the literature by using 2D planar fiber arrays [8] or 3D hexagonal or square fiber arrays [9-11]. In such perfect fiber networks, all the fibers are connected for load redistribution. Random local load sharing was modelled using imperfect fiber networks with random amounts of unconnected fibers [6]. Such imperfect networks were constructed by randomly deleting links between fibers, in a perfect triangular fiber array (figure 2). When a fiber breaks, the load it was carrying becomes carried by the surviving neighbouring fibers linked to it.

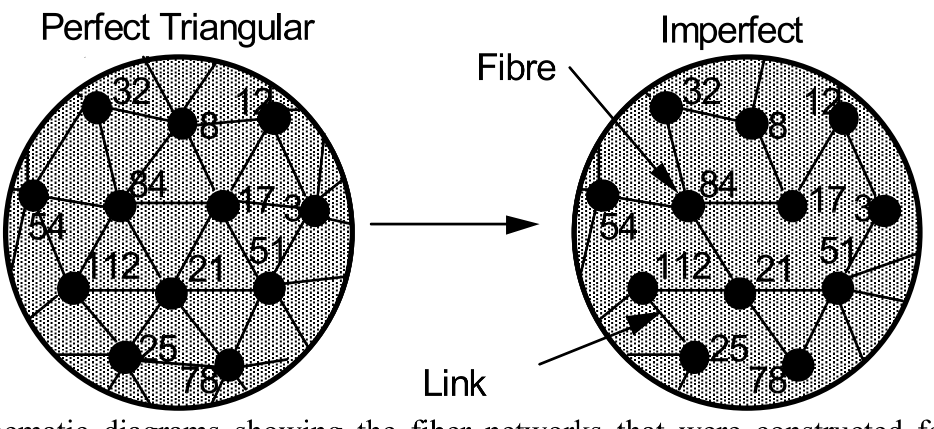

Figure 2 : Schematic diagrams showing the fiber networks that were constructed for the predictions of local load sharing effects on the ultimate failure of tows.

A random procedure was devised to generate imperfect networks [6], from a perfect triangular array of 500 fibers (SiC Nicalon tows). A randomly generated number (< 1) was assigned to each link (link index X_i) according to a random procedure. Deletion of a link was determined by the comparison of the link index X_i to the parameter β_r, β_r is the fraction of deleted links. Link i was deleted when $X_i \leq \beta_r$. Thus, when $\beta_r = 0$, no link was deleted. All the links were removed when $\beta_r = 1$. A percolation state is reached when $\beta_r = 0.5$ [12].

Simulations of the force strain-behavior were conducted using the above algorithm (previous section). When a fiber breaks, the load it was carrying is to be carried equally by the surviving neighbouring fibers linked to it. When a group of broken fibers is created (a cluster), the load is equally shared by the surviving fibers connected to the cluster. Ultimate failure is obtained when there is no surviving fiber connected to the cluster. Thus, when β_r = 1, fibers are not connected. Failure of the tow results from the failure of the weakest fiber : brittle failure of the tow.

500 computations were performed for each β_r value selected between 0 and 1 (β_r was increased by 0.01 increments) for the Nicalon NLM 202 fiber tows. The fiber statistical parameters are given in table 1.

2.4- Production of experimental data

The properties of SiC single fibers were determined using tensile tests performed on single filaments [13, 14] (table 1). The statistical parameters were estimated using the maximum Likelihood Estimator. The sample size (n) is indicated in table 1.

The tows were tested on a rigid frame machine. Details on specimen preparation and testing procedure can be found in [15, 16]. 20 Nicalon and 20 Hi-Nicalon specimens were prepared. Tow ends were glued within metal tubes that were then gripped into machine jaws. Tow elongation was measured using extensometers mounted on the grips. Measured deformations were corrected for load strain compliance.

	E (GPa)	m (-)	σ_o (MPa, $V_o = 1\ m^3$)	R_f (µm)
NLM 202 (n = 30)	180	4.6	8.4	7.25
Hi-Nicalon (n = 10)	280	5.2	29.0	6.75

Table 1 : Main characteristics of single SiC fibers [13, 14] (n is the number of samples).

3. RESULTS AND DISCUSSION

Figure 1 shows the typical force-strain behavior predicted by theory for the tows under strain-controlled conditions. The curves exhibit a non-linear force-strain relation associated to individual fiber breaks, and a small scatter (table 2).

Comparable curves were obtained experimentally. However, more or less pronounced load drops were present beyond maximum, indicative of unstable failures. In some cases, as shown on figure 1, the load drop was abrupt although strain-controlled conditions were prescribed, and much care had been taken during specimen preparation and mounting in order to avoid artifacts [16].

Figure 1 indicates that the experimental force-strain curves coincided with the first part of the predicted ones. A certain initial non linear domain was generally observed (figure 1). This domain reflects the presence of misaligned fibers. For the current particular value of the limit of the initial non linear deformation (0.25%) a negligible strength loss and a very small slack standard deviation ($\approx 5.10^{-4}$) were predicted [6].

Table 2 summarizes the data characterizing the maximum force and its scatter. Both the analytical model and the numerical simulations predicted identical results. A certain discrepancy between experimental data and predictions can be noticed. It thus appears that the maximum force was significantly overestimated by the model, whereas the scatter in experimental data was much larger than that predicted by theory.

	Experiments	Predictions (eq. 2, 3, 4)	Simulations (n_s = 100)
NLM 202	[13] (n=28, l=75 mm)	(m=4.6 σ_o=8.4 MPa)	(m=4.6 σ_o=8.4 MPa)
F_{max} (N)	77	94	95
$S(F_{max})$ (N)	8	2	2
C_v (%)	10	2	2
Hi-Nicalon	[17] (n=20, l=65 mm)	(m=5.2 σ_o=29.0 MPa)	(m=5.2 σ_o=29.0 MPa)
F_{max} (N)	146	165	167
$S(F_{max})$ (N)	6	3.4	3.1
C_v (%)	4	2	2

Table 2 : Comparison of the predicted and experimental data on failure of tows : NLM 202 and Hi-Nicalon. l = gauge length, n = sample size, n_s = number of simulations.

The maximum, minimum and average values of the sets of F_{max} that were determined for each value of β_r are plotted on figure 3. The load decrease from ELS to LLS (when β_r = 0) was drawn to be linear and continuous for simplicity. Several interesting features can be noticed from figure 3.

a - F_{max} decreases as RLLS conditions prevail. This trend is in agreement with logical expectation since local load sharing induces a larger fiber overloading when comparing to ELS. The amount of overloading is enhanced by β_r increases since the load is shared among a smaller number of fibers. A strength decrease has also been reported in the literature when comparing theory of ELS bundles and simulations for LLS conditions [11].

b - The scatter in F_{max} data increases in the presence of RLLS and when β_r increases.

c - The minimum value of F_{max} is logically obtained when β_r = 1: tow brittle failure (B.F.) is caused by the weakest fiber. The fiber strength derived from the corresponding mean F_{max} value (40 N) is 452 MPa. This value agrees with the lowest extreme in the distribution of SiC Nicalon fiber strength data [13].

d-The minimum values of F_{max} exhibit an erratic trend when $0.05 \leq \beta_r \leq 0.35$, which does not obey a classical law.

Table 3 shows that all the failure characteristics of SiC Nicalon tows (including standard deviation $S(F_{max})$ and coefficient of variation C_V) were predicted for β_r = 0.35, whereas a certain discrepancy with ELS based predictions is observed.

Table 3 : Comparison of predictions of ultimate failure of Nicalon NLM 202 tows with experimental results (n = number of testspecimens, l = gauge length).

	Experiment (n=28, l=75 mm)	ELS (m=4.6, σ_O=8.4MPa)	RLLS (m=4.6, σ_O=8.4 MPa, β_r= 0.35)
F_{max} (N)	77	94	76
$S(F_{max})$ (N)	8	2	7
C_V (%)	10	2	9

4. IMPLICATIONS IN COMPOSITE FAILURE

In textile CMCs, ultimate failure is caused by the failure of the weakest tow [1, 18]. Strengths of the weakest SiC Nicalon tows are given by the minimum value of F_{max} in figure 3. The tensile strength of a composite σ_{TS} can be estimated from tow strength (σ_{max}) using the following equations (tows and composite are assumed to have comparable lengths) :

$$\sigma_{TS} = V_L \, \sigma_{max} \tag{7}$$

$$\sigma_{max} = \frac{F_{max}}{N_t(1-\alpha(\sigma_{max})\pi R_f^2} \tag{8}$$

where V_L is the volume fraction of longitudinal fiber tows.

σ_{TS} values were predicted for 2D SiC Nicalon tow reinforced composites, for N_t = 500, R_f = 7.5 µm, $\alpha(\sigma_{max})$ = 0.17 and $V_L \approx 0.2$. Table 4 shows that σ_{TS} derived for ELS is in good agreement with the strengths measured on 2D Nicalon/SiC composites (figure 4) [18, 19], whereas σ_{TS} obtained for LLS significantly underestimates composite failure. These results are consistent with the failure mechanism proposed for 2D Nicalon/SiC composites which involves completely debonded tows, fiber failures and global load sharing after matrix cracking saturation [1, 20].

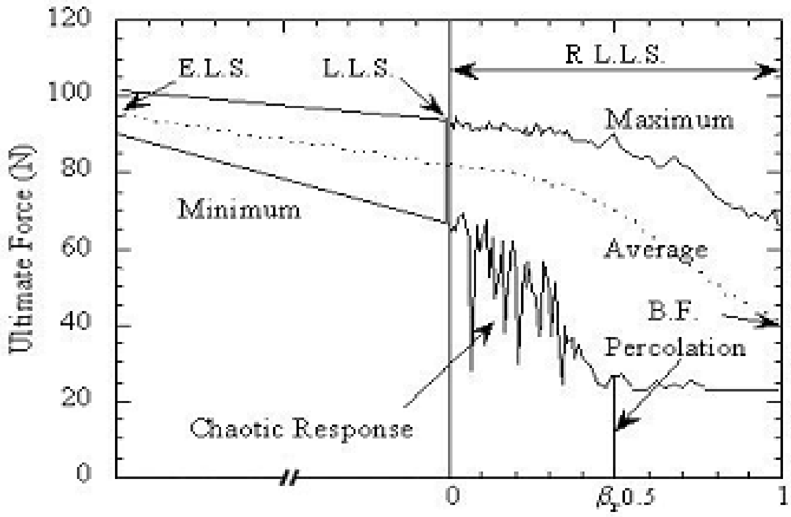

Figure 3 : Influence of local load sharing conditions on tow maximum forces (F_{max}) predicted for Nicalon NLM 202 tows. (B.F. = Brittle failure).

Furthermore, it is worth pointing out that σ_{TS} obtained for brittle tow failure (β_r = 1), coincides with the proportional limit of 2D Nicalon/SiC (figure 4), and with the strength of those brittle 2D Nicalon/SiC composites obtained with strong fiber/matrix bonds. Finally, it is worth noticing that σ_{TS} decreases significantly as LLS or RLLS operate in tows. This trend reflects the variability in composite strengths induced by reproducibility in fiber matrix bonds in manufactured composites. Furthermore, this trend also illustrates composite embrittlement as oxide fiber bonding grows in oxidizing environments at high temperatures.

Table 4 : Composite strengths estimated from the resistances to failure of SiC Nicalon multifilament tows.

	F_{max} (N)	Predicted σ_{TS} (MPa)
ELS	90	245
LLS	70	190
RLLS ($\beta_r = 0.35$)	40	109
RLLS ($\beta_r = 1$)	25	68

Finally, it is worth pointing out that the features in ultimate strengths discussed in a previous paper [18] for 2D Nicalon/SiC composites are consistent with those displayed by the minimum values of F_{max} in figure 3. In particular, the non-ordered successive failures and the limited size effects that were evidenced [18] may be related to the erratic trend shown on figure 3.

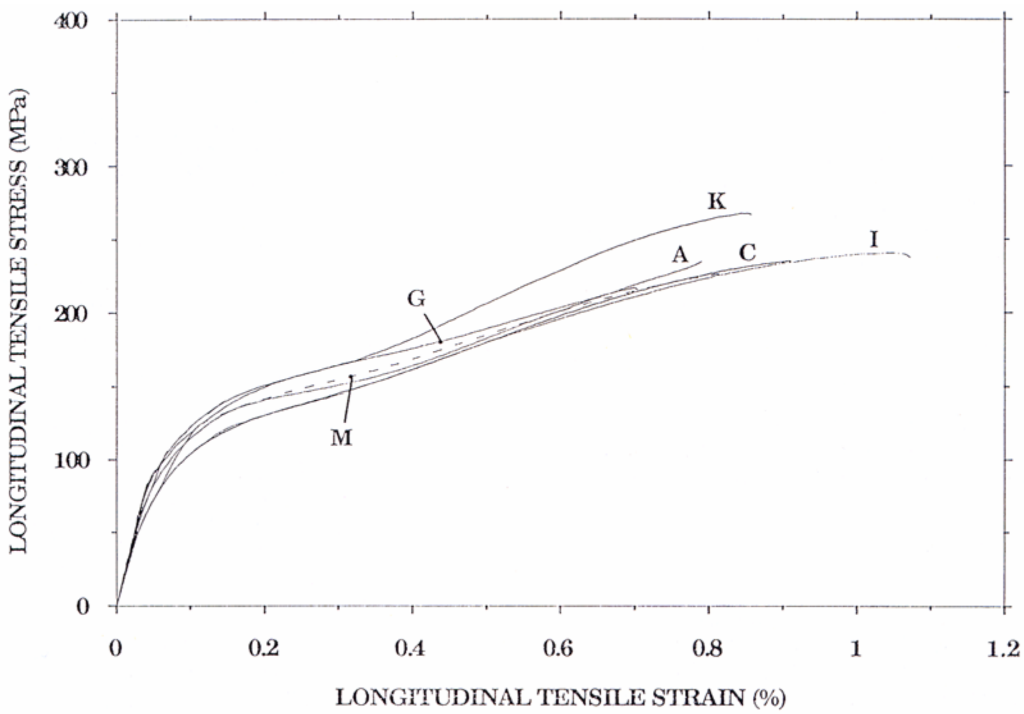

Figure 4 : Tensile stress-strain behavior in tension measured on 2D SiC/SiC composites reinforced with as fabricated Nicalon multifilament tows.

5. CONCLUSION

The experimental force-strain behavior of tows of Nicalon and Hi-Nicalon fibers exhibited a certain discrepancy with that one predicted by theory :

- features of catastrophic failure were observed although strain-controlled conditions were prescribed.
- an unexpected significant scatter in tow strength data was obtained,
- the tow strengths were smaller than those predicted from fiber properties.

Local load sharing induces a drop in tow strengths, and an enhanced scatter in data when comparing to equal load sharing conditions. Taking into account randomt local load sharing allowed sound predictions of tow strengths and associated scatter.

Tow strength data are preponderantly influenced by extrinsic factors. However testing of tows is an interesting technique to determine fiber properties, provided the first part of the force-strain curve below maximum is considered. Typical features associated to scatter in tow strengths, and more particularly distribution of minimum tow strength data are probably of significance for the analysis of ultimate failure of textile ceramic matrix composites.

REFERENCES

1- **Lamon**, **J**., "A micromechanics-based approach to the mechanical behavior of brittle-matrix composites," *Composites Science and Technology*, **61** (2001) 2259-2272.
2- **Daniels**, **H.E**., "The statistical theory of the strength of bundles of threads I, *Proc. Royal Soc.,* **A183** (1945) 405-435.
3- **Coleman**, **B.D**., "On the strength of classical fibers and fibers bundle," *J. Mech. Phys. Solid*, **7** (1958) 60-70.
4- **Phoenix**, **S.L**. and **Taylor**, **H.M**., "The asymptotic strength distribution of a general fiber bundle," *Adv. Appl. Prob*., **5** (1973) 200-216.
5- **Phoenix**, **S.L**., "Probabilistic strength analysis of fiber bundles structures," *Fiber Science and Technology*, **7** (1974) 15-31.
6- **Calard**, **V**., **Lamon**, **J**., Failure of bundles, *Composites Science and Technology*, **64** (2004) 701-710.
7- **R'Mili**, **M**., **Murat**, **M**., "Caractérisation des fibres par amélioration de l'essai sur mèche avec mesure directe de la déformation," *C.R. Acad. Sci. Paris*, **324**/II b (1997) 355-364.
8- **Harlow**, **D.G**., "Probabilistic models for the tensile strength of composite materials," D. Phil. Thesis, Cornell University, USA (1977).
9- **Batdorf**, **S.B**., "Tensile strength of unidirectionally reinforced composites," *J. Reinforced Plast. & Comp*., **1** (1982) 153-163.
10- **Hedgepeth**, **J.M**., **Van Dyke**, **P**., "Local stress concentrations in imperfect filamentary composite materials," *J. Composite Materials*, **1** (1967) 294-309.
11- **Mahesh**, **S**., **Phoenix**, **S.L**., **Beyerlein**, **I**., "Strength distributions and size effects for 2D and 3D composites with Weibull fibers in an elastic matrix," *International Journal of Fracture*, **115** (2002) 41-85.
12- **Stauffer**, **D**., "Scaling theory of percolation clusters," *Physics Reports (Review Section of Physics Letters)*, **54**/1 (1979) 1-79.
13- **Lissart**, **N**., **Lamon**, **J**., "Statistical analysis of failure of SiC fibers in the presence of bimodal flaw populations", *J. Mat. Sci*. **32** (1997) 6107-6117.
14- **Bertrand**, **S**., "Durée de vie de matériaux composites à matrice céramique et interphase nanoséquencée", PhD Thesis, n° 1927, University of Bordeaux 1, France, 1994.
15- (ENV 1007-5), « Advanced technical ceramic-ceramic composites – methods of test for reinforcements – Part 5 : Determination of distribution of tensile strength and tensile strain to failure of filaments within a multifilament tow at ambient temperature » European Committee for Standardization, CEN/TC 184/SC 1, Brussel, 1997.
16- **Lissart**, **N**., **Lamon**, **J**., « Evaluation des propriétés de monofilaments à partir d'essais de traction sur mèches », Comptes-rendus des 9° Journées Nationales sur les Composites (JNC 9), edited by J.P. Favre and A. Vautrin , AMAC, 2, (1994) 589-598.
17- **Pastor**, **K**., « Propriétés mécaniques et rupture de fils et de fibres céramiques Hi-Nicalon », DEA Report, University of Bordeaux 1, France, 1997.

18- **Calard**, **V**., **Lamon**, **J**., "A probabilistic approach to the ultimate failure of ceramic-matrix composites – part I : experimental investigation of 2D woven SiC/SiC composites," *Composites Science and Technology*, **62**/3 (2002) 385-393.
19- **Droillard**, **C**., **Lamon**, **J**., "Fracture toughness of 2D woven SiC/SiC CVI-composites with multilayered interphases," *J. Am. Ceram. Soc.*, **79**/4 (1996) 849-858.
20- **Lissart**, **N**., **Lamon**, **J**., "Damage and failure in ceramic matrix minicomposites: experimental study and model," *Acta Mater*., **45**/3 (1997) 1025-1044.